10. Tuschl, T., Zamore, P. D., Lehmann, R., Bartel, D. P. & Sharp, P. A. Targeted mRNA degradation by double-stranded RNA *in vitro*. *Genes Dev.* **13,** 3191–3197 (1999).
11. Montgomery, M. K., Xu, S. & Fire, A. RNA as a target of double-stranded RNA-mediated genetic interference in *Caenorhabiditis elegans*. *Proc. Natl Acad. Sci. USA* **95,** 15502–15507 (1998).
12. Fire, A. *et al.* Potent and specific genetic interference by double-stranded RNA in *Caenorhbditis elegans*. *Nature* **391,** 806–810 (1998).
13. Olsen, P. H. & Ambros, V. The lin-4 regulatory RNA controls developmental timing in *Caenorhabditis elegans* by blocking LIN-14 protein synthesis after the initiation of translation. *Dev. Biol.* **216,** 671–680 (1999).
14. Tabara, H. *et al.* The rde-1 gene, RNA interference, and transposon silencing in *C. elegans*. *Cell* **99,** 123–132 (1999).

Acknowledgements

We thank the following people for RNA and tissue samples: T. Heanue, R. Pearse and C. Tabin for chick; J. Gerhart and M. Kirschner for *Xenopus* and acorn worm; S. Agarwal for *Xenopus*; N. Stavropoulos for mouse; C. Unabia and K. del Carmen for annelid and mollusc; H. Bode for Hydra; J. Nardone and S. Ferrari for *Arabidopsis*; P. Sudarsanam for yeast; and D. Selinger for *E. coli*. The phylogenetic survey in this work was inspired by the NASA Evolution and Development meetings organized by E. Davidson and C. Golden. This work was supported by an NIH grant from NIGMS to G.R. and a grant from the MGH Fund for Medical Discovery to A.E.P.

Correspondence and requests for materials should be addressed to G.R.

Polarization of the anterior–posterior axis of *C. elegans* is a microtubule-directed process

Matthew R. Wallenfang & Geraldine Seydoux

Department of Molecular Biology and Genetics, Johns Hopkins University School of Medicine, Baltimore, Maryland 21205, USA

In *Caenorhabditis elegans*, polarity along the anterior–posterior (A/P) axis is established shortly after fertilization and is determined by the sperm, whose position specifies the posterior end of the embryo[1]. Although many factors required for the establishment of A/P polarity have been described[2,3], the nature of the spatial cue provided by the sperm remains unknown. Here we show that a microtubule-organizing centre is necessary and sufficient to establish several aspects of A/P polarity. In wild-type embryos, appearance of the first molecular asymmetries along the A/P axis correlates with and requires nucleation of microtubules by the sperm-derived centrosomes (sperm asters). In mutant embryos arrested in meiosis, sperm asters fail to form, and posterior is defined by the position of the persistent meiotic spindle rather than by the position of the sperm. Together, our data indicate that the primary spatial cue for A/P polarity in *C. elegans* derives from microtubules emanating from the sperm asters. Our findings support a parallel[4–7] between *C. elegans* zygotes and other cells, such as *Drosophila* oocytes, which rely on microtubules to regulate polarity.

Caenorhabditis elegans oocytes appear to have no predetermined A/P polarity[1]. The first manifestations of polarity are seen roughly 30 min following fertilization, after the oocyte chromatin, which had been arrested in prophase of meiosis I, completes meiosis. At that time, several proteins become localized asymmetrically along the long axis of the embryo: in particular, PAR-2 localizes to the cortex nearest the sperm pronucleus (future posterior end), and PAR-3 localizes in a reciprocal pattern on the cortex opposite the sperm pronucleus[2] (future anterior end; Fig. 1a). Each of these is required to localize the PAR-1 kinase to the posterior cortex. PAR-1, in turn, is required for the asymmetric segregation of several factors in the cytoplasm, including PIE-1 and the germline-specific P granules which localize to the posterior[2] (Fig. 1a). Segregation of P granules has been correlated with an internal flow of cytoplasm directed towards the sperm pronucleus, which also occurs during this period[8,9] (Fig. 1a). The sperm pronucleus itself is dispensable for polarity[10], leaving open the question of which sperm-derived component is responsible for polarizing the embryo.

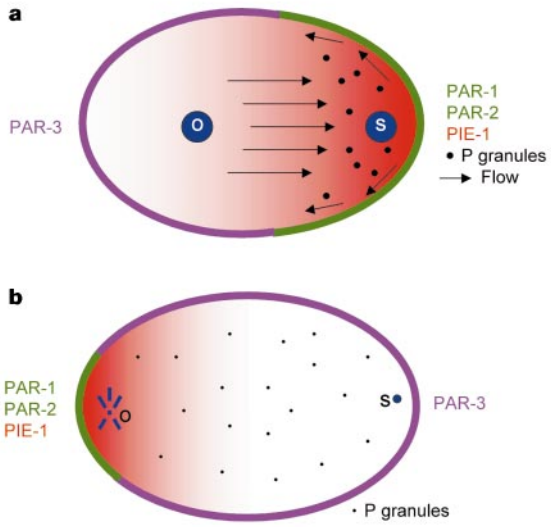

Figure 1 Establishment of A/P polarity in *C. elegans*. **a**, Polarity in wild-type embryos. Embryo is shown in first mitotic prophase during pronuclear migration. In most fertilization events, sperm entry occurs on the side opposite the oocyte nucleus[1]. In this and Figs 2 and 3, the position of the oocyte chromatin is indicated by an 'O' and that of the sperm chromatin by an 'S' (in some figures, the sperm chromatin is not visible in the focal plane shown). Arrows indicate cytoplasmic flow, which flows towards the sperm pronucleus in the interior of the embryo and away from it along the cortex. Shown are the asymmetric distributions of PAR-1 and PAR-2 (green), PAR-3 (magenta), PIE-1 (red) and P granules (dots). **b**, Polarity in *mat* mutant embryos. The oocyte chromatin is arrested in metaphase of meiosis I and the sperm chromatin remains condensed.

To address this question, we have analysed a collection of temperature sensitive mutants (*mat-1*, *mat-2*, *mat-3*, *emb-27*, *emb-30)* that arrest shortly after fertilization while the oocyte chromatin is in metaphase of meiosis I (A. Golden, P. Sadler, M.R.W., G.S. and D. Shakes, manuscript in preparation). Consistent with their metaphase arrest phenotype, *mat-1* and *emb-30* encode *C. elegans* homologues of the anaphase-promoting complex (APC) components Cdc27 (J. Schumacher, D. Shakes and A. Golden, personal communication) and APC4/Lid1 (ref. 11), respectively.

Because fertilization usually occurs opposite the oocyte nucleus, mutant embryos in this collection arrest with the oocyte chromatin in meiosis at one end of the embryo and condensed sperm chromatin at the other end (Fig. 1b). To determine whether A/P polarity can be established under these conditions, we determined the distribution of PIE-1, which in wild type segregates towards the sperm pronucleus after meiosis is completed. We observed asymmetric PIE-1 in 48% of *mat-1* mutant embryos (Table 1). Notably, when asymmetric, PIE-1 always was enriched on the side of the oocyte chromatin rather than on the sperm side (Fig. 2a). Similar results were obtained with the other mutants (Table 1). Examination of live embryos expressing a PIE-1–GFP (green fluorescent protein) fusion showed that PIE-1 becomes asymmetric in all *mat-1* embryos (Fig. 2b); however, this asymmetry is transient, causing it to be observed in only 48% of embryos in asynchronous populations (Table 1).

Immunostaining with PAR-1, PAR-2 and PAR-3 antibodies showed that PAR asymmetry is also 'reversed' in *mat-1* mutants: PAR-1 and PAR-2, which in wild type localize to the cortex nearest the sperm, were on the cortex nearest the oocyte chromatin in *mat-1*

embryos (Table 1; and data not shown); and PAR-3, which in wild type localizes to the cortex opposite the sperm, was on the cortex opposite the oocyte chromatin in *mat-1* embryos (Table 1). As in wild type[12,13], PIE-1 asymmetry was dependent on *par-1* and *par-3* activities in *mat-1* mutants, and PAR-3 asymmetry was independent of *par-1* (Table 1). These observations indicate that, even though A/P polarity appears 'reversed' in *mat-1* embryos, the PAR hierarchy required to establish polarity in wild type is maintained in these mutants.

In contrast to the PARs and PIE-1, P granules remained uniformly distributed in *mat-1* embryos (Table 1). P granules in these mutants remained small and dispersed (Fig. 2c), as they appear in wild-type oocytes and newly fertilized embryos. Cytoplasmic flow, which in wild type has been correlated with P-granule segregation[9], was also not observed in *mat-1* embryos (4 out of 4 embryos; see Methods). We conclude that, although completion of meiosis is not required for the establishment of PAR and PIE-1 asymmetries, it is required for P-granule segregation and cytoplasmic flow.

To understand the basis of the apparent reversal of PAR/PIE-1 asymmetry in *mat-1* embryos, we examined the distributions of PAR-2 and PAR-3 with respect to the location of the meiotic spindle. We found that localization of these proteins always was correlated (PAR-2) or inversely correlated (PAR-3) with the position of the meiotic spindle, even when the meiotic spindle was located off centre relative to the pole (Fig. 2d–f). In rare embryos (<1%), an additional patch of PAR-2 was sometimes observed away from the meiotic spindle. In all cases (5 out of 5), these ectopic patches were associated with foci of microtubules that appeared to have formed spontaneously in the cytoplasm, away from the oocyte and sperm chromatin (Fig. 2g).

These observations indicated that the meiotic spindle, rather than the sperm, may act as the main polarizing cue in embryos arrested in meiosis. To test this hypothesis further, we examined the consequence of disrupting the meiotic spindle in *mat-1* embryos. Treatment of *mat-1* embryos with the microtubule-depolymerizing drug nocodazole disrupted the integrity of the meiotic spindle (see Methods) and reduced the number of embryos with asymmetric PAR-2 (Table 1). To block formation of the meiotic spindle completely, we used RNA-mediated interference (RNAi) against *ncc-1*, a *C. elegans* cdc2 homologue required for entry into M phase[14]. *mat-1;ncc-1* embryos did not form a meiotic spindle and did not segregate PIE-1 (Table 1). These data are consistent with the meiotic spindle acting as the primary polarizing cue in *mat-1* mutants.

This finding raised the possibility that an eccentrically located microtubule-organizing centre might be sufficient to polarize the *C. elegans* embryo along its A/P axis. In wild-type embryos, the sperm-derived centrosomes begin to nucleate microtubules around the sperm pronucleus (sperm asters) after the completion of meiosis[15], and thus potentially could function as the polarity cue[1,8,10]. To explore this hypothesis, we stained wild-type embryos expressing a PAR-2–GFP fusion with an antibody against α-tubulin (Fig. 3a–d). During meiosis (Fig. 3a), and immediately afterwards before sperm aster formation (Fig. 3b), PAR-2 was present at low levels uniformly throughout the cytoplasm and weakly at the cortex. Asymmetric PAR-2 was first detected on the cortex nearest the male pronucleus when sperm asters first became visible (Fig. 3c). A similar correlation was observed with PAR-1, PAR-3 and PIE-1 (data not shown). During sperm aster growth, the domain occupied by PAR-2 on the cortex expanded until reaching close to 50% embryo length by pronuclear meeting (data not shown). In later stages, during formation of the mitotic spindle, PAR-2 did not extend further (Fig. 3d), perhaps limited by the presence of PAR-3 in the anterior[12,16].

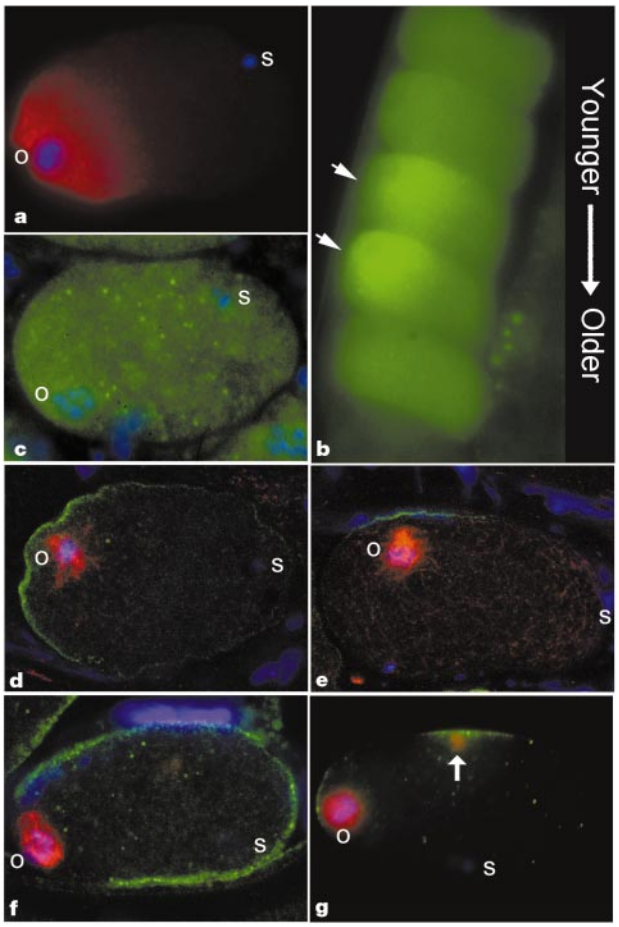

Figure 2 A/P polarity in *mat* mutant embryos. **a**, *mat-1*(*ax227*) embryo immunostained for PIE-1 (red) and DAPI (blue). **b**, Embryos inside the uterus of a *mat-1*(*ax227*) hermaphrodite expressing PIE-1–GFP (green). Embryos are arranged from youngest to oldest (top to bottom). All are in the one-cell stage; those with asymmetric PIE-1 are indicated by arrows. A similar pattern was observed in all hermaphrodites examined ($n > 50$), indicating that PIE-1 segregates transiently in all mutant embryos. **c**, *mat-1(ax227)* embryo immunostained for P granules (green) and DAPI (blue). This same embryo segregated PIE-1 towards the side of the oocyte chromatin (not shown). **d**, **e**, *mat-1*(*RNAi*) embryos expressing PAR-2–GFP (green) immunostained for α-tubulin (red) and DAPI (blue). **f**, *mat-1(ax227)* embryo immunostained for PAR-3 (green), α-tubulin (red) and DAPI (blue). **g**, *mat-1(ax227)* embryo immunostained for PAR-2 (green), α-tubulin (red) and DAPI (blue). Arrow points to an ectopic focus of microtubules.

Table 1 Asymmetric segregation in *mat* mutants

Protein scored	Genotype/treatment	% Asymmetric* (*n*)
PIE-1	*mat-1*(*ax227*)	48 (114)
PIE-1	*mat-2*(*ax76*)	39 (52)
PIE-1	*mat-3*(*ax148*)	45 (64)
PIE-1	*emb-27*(*ax81*)	42 (99)
PIE-1	*emb-30*(*ax69*)	38 (60)
PIE-1	*mat-1*(*RNAi*)	46 (84)
PIE-1	*mat-1*(*RNAi*); *par-1*(*b274*)	0 (27)
PIE-1	*mat-1*(*RNAi*); *par-3*(*e2074*)	3 (136)
PAR-2	*mat-1*(*ax227*)†	39 (247)
PAR-2	*mat-1*(*ax227*); nocodazole	21 (113)
PAR-3	*mat-1*(*RNAi*)	48 (42)
PAR-3	*mat-1*(*RNAi*); *par-1*(*b274*)	43 (21)
P granules‡	*mat-1*(*ax227*)	0 (32)
PIE-1:GFP	*mat-1*(*ax227*)	45 (55)
PIE-1:GFP	*mat-1*(*ax227*); *ncc-1*(*RNAi*)	0 (66)
PIE-1:GFP	*mat-1*(*ax227*); *air-1*(*RNAi*)	46 (67)

*Per cent of embryos in which the indicated protein/marker was asymmetric. All other embryos showed uniform distribution. When asymmetric, the protein assayed always was found enriched on the side of the oocyte chromatin (as identified by DAPI staining), except for PAR-3 which segregated to the side opposite the oocyte chromatin.
†These embryos were prepared in the same manner as the nocodazole treated embryos (see Methods) except that nocodazole was omitted.
‡P granules could not be detected in 55% of *mat-1*(*ax227*) embryos. Only embryos with visible P granules were included in our analysis.

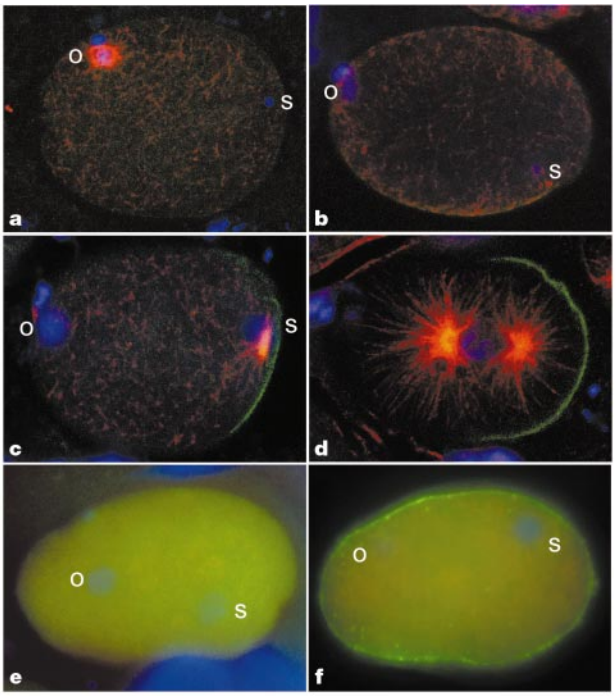

Figure 3 Establishment of A/P polarity in wild type correlates with and requires sperm aster formation. **a**–**d**, Wild-type one-cell embryos expressing PAR-2–GFP (green) immunostained for α-tubulin (red) and DAPI (blue). **a**, Meiosis II; **b**, end of meiosis; **c**, sperm aster formation; **d**, mitotic pro-metaphase (oocyte and sperm pronuclei have fused). **e**, *air-1*(*RNAi*) embryo expressing PIE-1–GFP (green) and immunostained for α-tubulin (red, diffuse due to lack of sperm asters) and DAPI (blue). **f**, *air-1*(*RNAi*) embryo immunostained for α-tubulin (red, diffuse), PAR-3 (green) and DAPI (blue).

Previous studies using microtubule inhibitors failed to determine a role for sperm asters in the establishment of polarity[8,17]. Those studies, however, were performed in one-cell embryos that had completed pronuclear formation, and thus potentially did not address the possibility that sperm asters might be involved in establishing polarity at an earlier stage[8,17]. To test this possibility, we disrupted sperm aster formation by interfering with *air-1* expression. *air-1* belongs, along with *Drosophila* Aurora and *Saccharomyces cerevisiae* Ipl1, to a subfamily of serine/threonine kinases that regulate spindle dynamics during mitosis[18]. Disruption of *air-1* expression by RNAi has been reported to disrupt PIE-1 localization[18]. We found that this defect correlates with a block in the formation of sperm asters. *air-1*(*RNAi*) embryos could be divided into two classes: embryos with no detectable asters (42%, 33/79); and embryos with small but distinct asters (58%, 46/79). Among the first class, 91% of embryos failed to localize PIE-1 (Fig. 3e). These embryos also had uniform PAR-3 at the cortex confirming that A/P polarity had not been established (Fig. 3f). In contrast, 80% of *air-1*(*RNAi*) embryos that had retained asters segregated PIE-1 and PAR-3. To confirm that the *air-1* A/P polarity defect was due to a lack of sperm asters, we examined the requirement for *air-1* in *mat-1* embryos where polarity is established independently of sperm asters. *mat-1;air-1* embryos were able to segregate PIE-1 to the same extent as *mat-1* embryos (Table 1), confirming that AIR-1 itself is not required to establish A/P polarity. We conclude that establishment of A/P polarity in wild-type embryos is dependent on sperm aster formation. A similar conclusion has been reached following a study[19] showing that mutations in *spd-2*, which delay and attenuate sperm aster formation, eliminate A/P polarity in wild type.

Together, our results show that a microtubule-organizing centre is necessary, and can be sufficient, to establish many aspects of A/P polarity in *C. elegans* embryos. We propose that when microtubules emanating from such a centre reach the cortex, they, or factors associated with them, affect the local balance between PAR-2 and PAR-3, perhaps by promoting binding of PAR-2 to the cortex and/or by inhibiting binding of PAR-3. This interaction may be dependent on the actin cytoskeleton, which is required for A/P polarization[17,20]. We propose that under normal circumstances only microtubules nucleated by the sperm asters reach the cortex. Meiotic microtubules remain confined to the spindle, unless allowed to persist for a prolonged period as occurs in embryos arrested in meiosis. Indeed, meiotic spindles in *mat* mutants have a characteristic frayed appearance not seen in wild type (compare Fig. 2d–g with Fig. 3a).

One question raised by our studies is whether the initial point of contact between microtubules and cortex serves as a nucleation site from which posterior markers can spread, or whether microtubule–cortex interactions are required all along the posterior half of the embryo to define the complete PAR-2 domain. In support of the latter possibility, we have noted that PAR-2 domains are smaller in *mat* mutants than in wild type (compare Fig, 2d, e with Fig. 3d), suggesting that sperm aster growth is required for expansion of the PAR-2 domain. Alternatively or additionally, PAR-2 domain expansion could depend on actin-based mechanisms that fail to occur in *mat* embryos, such as cytoplasmic flow. Indeed, small PAR-2 domains have also been observed in embryos deficient for the non-muscle myosin II regulatory light chain, *mlc-4* (ref. 21), suggesting that refinement of PAR domains may require mechanisms distinct from those used for their establishment.

A homologue of PAR-1 has been shown to function in the establishment of A/P polarity in *Drosophila* oocytes[4,5], a process dependent on polarization of the microtubule cytoskeleton[22]. PAR-1-like kinases also exist in mammals where they have been implicated in regulating microtubule dynamics and epithelial cell polarity[23,24]. Together with these studies, our finding that A/P polarity in *C. elegans* is initiated by microtubules supports the idea that conserved microtubule and PAR-1 dependent mechanisms regulate polarity in cells as diverse as *C. elegans* zygotes, *Drosophila* oocytes and mammalian epithelial cells. □

Methods

Strains and alleles

We used the following strains: N2 (wild type), *axIs73*(pJH3.92, pRF4), *axEx1094*(pMW1.03, pRF4), *mat-1*(*ax227ts*)I, *mat-1*(*ax227ts*)I; *axIs73*(pJH3.92, pRF4), *mat-2*(*ax76ts*)II, *mat-3*(*ax148ts*)III, *emb-27*(*ax81ts*)II, *emb-30*(*ax69ts*)III, *rol-4*(*sc8*) *par-1*(*b274*)IV/*nT1* (IV; V), *lon-1*(*e185*) *par-3*(*e2074*) III; and *sDp3* (III; f). *axIs73* is an integrated array containing a PIE-1–GFP transgene[25]. *axEx1094* is an extrachromosomal array containing a PAR-2–GFP fusion under the control of the PIE-1 promoter. This transgene is expressed in early embryos in the same pattern as endogenous PAR-2 (data not shown). We isolated the *ax* alleles used in this study in a large-scale screen for temperature-sensitive embryonic lethal mutations (M.R.W. and G. S., unpublished data). Embryos arrested in meiosis were derived from mutant hermaphrodites that had been shifted as adults to the non-permissive temperature (25 °C) for 8–12 h. Under these conditions, only oocyte meiosis is affected; sperm meiosis, which in hermaphrodites occurs during larval development, is not affected.

Immunofluorescence microscopy

We used the following antibodies: anti-PIE-1 (ref. 13), anti-PAR-1 (ref. 26), anti-PAR-2 (ref. 16), anti-PAR-3 (ref. 12), anti-P granule[27] and anti-α-tubulin (mAbE7, Developmental Studies Hybridoma Bank; or DM1A, Sigma). Immunostaining was done as described[13] using DAPI (4′,6-diamidino-2-phenylindole dihydrochloride) to visualize oocyte and sperm DNA. We carried out analysis using either a compound fluorescence microscope (Zeiss Axioplan 2) or laser scanning confocal microscope (Zeiss LSM 510).

RNA interference

Double-stranded RNAi was used to knock out gene function using the bacterial feeding method[28]. Targeted DNAs were cloned into the feeding vector L4440, transformed into *Escherichia coli* H115(DE3), and the resulting transformants were used to spread NGM plates containing 60 μg ml^{-1} ampicillin and 80 μg ml^{-1} IPTG. Bacterial lawns grown overnight were used immediately or stored at 4 °C for up to 3 weeks. Hermaphrodites were placed on bacterial lawns as L4 larvae and allowed to feed for 20–30 h at 25 °C before their embryos were examined.

Drug treatments

Gravid adult hermaphrodites were placed onto slides into 8 μl of egg salts[29] containing 10 μg per ml nocodazole (Sigma) in DMSO (0.1% final concentration) and cut open with a syringe needle to release embryos. Slides were incubated in a humid chamber for 15–20 min before processing for immunostaining with anti-PAR-2 and anti-α-tubulin antibodies as described above. This treatment severely disrupted the meiotic spindle in most embryos but was not sufficient to eliminate it entirely (data not shown).

Time-lapse videomicroscopy

Young adult hermaphrodites were anaesthetized in 0.1% tricaine, 0.01% tetramisole in M9 (ref. 30), placed on a 2% agarose pad and covered with a cover slip. We recorded time-lapse movies of embryos *in utero* from fertilization to first cleavage (~45 min) for wild-type embryos, and from fertilization to 75 min after fertilization for *mat-1* embryos, using a Zeiss Axioplan 2 equipped with a DAGE video camera and Scion LG3 frame grabber. Nomarski images were acquired every 3 s using the 4D grabber software (Laboratory for Optical and Computational Instrumentation, University of Wisconsin, Madison). Resulting Quicktime movies were analysed for directed cytoplasmic flow by following the movement of yolk granules as described[8]. In two of the 4 *mat-1* embryos analysed, we also examined PAR-2–GFP fluorescence at the end of the movie and confirmed that it had become asymmetric.

Received 10 May; accepted 16 August 2000.

1. Goldstein, B. & Hird, S. N. Specification of the anteroposterior axis in *Caenorhabditis elegans*. *Development* **122,** 1467–1474 (1996).
2. Rose, L. S. & Kemphues, K. J. Early patterning of the *C. elegans* embryo. *Annu. Rev. Genet.* **32,** 521–545 (1998).
3. Bowerman, B. Maternal control of pattern formation in early *Caenorhabditis elegans* embryos. *Curr. Top. Dev. Biol.* **39,** 73–117 (1998).
4. Shulman, J. M., Benton, R. & St Johnston, D. The *Drosophila* homolog of *C. elegans* PAR-1 organizes the oocyte cytoskeleton and directs oskar mRNA localization to the posterior pole. *Cell* **101,** 377–388 (2000).
5. Tomancak, P. *et al.* A *Drosophila melanogaster* homologue of *Caenorhabditis elegans* par-1 acts at an early step in embryonic-axis formation. *Nature Cell Biol.* **2,** 458–460 (2000).
6. Kemphues, K. PARsing embryonic polarity. *Cell* **101,** 345–348 (2000).
7. Morris, J., Lehmann, R. & Navarro, C. PARallels in axis formation. *Science* **288,** 1759–1760 (2000).
8. Hird, S. N. & White, J. G. Cortical and cytoplasmic flow polarity in early embryonic cells of *Caenorhabditis elegans*. *J. Cell Biol.* **121,** 1343–1355 (1993).
9. Hird, S. N., Paulsen, J. E. & Strome, S. Segregation of germ granules in living *Caenorhabditis elegans* embryos: cell-type-specific mechanisms for cytoplasmic localisation. *Development* **122,** 1303–1312 (1996).
10. Sadler, P. L. & Shakes, D. C. Anucleate *Caenorhabditis elegans* sperm can crawl, fertilize oocytes and direct anterior-posterior polarization of the 1-cell embryo. *Development* **127,** 355–366 (2000).
11. Furuta, T. *et al.* EMB-30: An APC4 homologue required for metaphase-to-anaphase transitions during meiosis and mitosis in *Caenorhabditis elegans*. *Mol. Biol. Cell* **11,** 1401–1419 (2000).
12. Etemad-Moghadam, B., Guo, S. & Kemphues, K. J. Asymmetrically distributed PAR-3 protein contributes to cell polarity and spindle alignment in early *C. elegans* embryos. *Cell* **83,** 743–752 (1995).
13. Tenenhaus, C., Schubert, C. & Seydoux, G. Genetic requirements for PIE-1 localization and inhibition of gene expression in the embryonic germ lineage of *Caenorhabditis elegans*. *Dev. Biol.* **200,** 212–224 (1998).
14. Boxem, M., Srinivasan, D. G. & van den Heuvel, S. The *Caenorhabditis elegans* gene ncc-1 encodes a cdc2-related kinase required for M phase in meiotic and mitotic cell divisions, but not for S phase. *Development* **126,** 2227–2239 (1999).
15. Albertson, D. G. Formation of the first cleavage spindle in nematode embryos. *Dev. Biol.* **101,** 61–72 (1984).
16. Boyd, L., Guo, S., Levitan, D., Stinchcomb, D. T. & Kemphues, K. J. PAR-2 is asymmetrically distributed and promotes association of P granules and PAR-1 with the cortex in *C. elegans* embryos. *Development* **122,** 3075–3084 (1996).
17. Strome, S. & Wood, W. B. Generation of asymmetry and segregation of germ-line granules in early *C. elegans* embryos. *Cell* **35,** 15–25 (1983).
18. Schumacher, J. M., Ashcroft, N., Donovan, P. J. & Golden, A. A highly conserved centrosomal kinase, AIR-1, is required for accurate cell cycle progression and segregation of developmental factors in *Caenorhabditis elegans* embryos. *Development* **125,** 4391–4402 (1998).
19. O'Connell, K., Maxwell, K. & White, J. The spd-2 gene is required for polarization of the anteroposterior axis and formation of the sperm asters in the *Caenorhabditis elegans* zygote. *Dev. Biol.* **221,** 55–70 (2000).
20. Hill, D. P. & Strome, S. Brief cytochalasin-induced disruption of microfilaments druing a critical interval in one-cell *C. elegans* embryos alters the partitioning of developmental instructions to the two-cell embryo. *Development* **108,** 159–172 (1990).
21. Shelton, C. A., Carter, J. C., Ellis, G. C. & Bowerman, B. The nonmuscle myosin regulatory light chain gene mlc-4 is required for cytokinesis, anterior-posterior polarity, and body morphology during *Caenorhabditis elegans* embryogenesis. *J. Cell Biol.* **146,** 439–451 (1999).
22. van Eeden, F. & St Johnston, D. The polarisation of the anterior-posterior and dorsal-ventral axes during *Drosophila* oogenesis. *Curr. Opin. Genet. Dev.* **9,** 396–404 (1999).
23. Bohm, H., Brinkmann, V., Drab, M., Henske, A. & Kurzchalia, T. V. Mammalian homologues of *C. elegans* PAR-1 are asymmetrically localized in epithelial cells and may influence their polarity. *Curr. Biol.* **7,** 603–606 (1997).
24. Drewes, G., Ebneth, A., Preuss, U., Mandelkow, E. M. & Mandelkow, E. MARK, a novel family of protein kinases that phosphorylate microtubule-associated proteins and trigger microtubule disruption. *Cell* **89,** 297–308 (1997).
25. Reese, K. J., Dunn, M. A., Waddle, J. A. & Seydoux, G. Asymmetric segregation of PIE-1 in *C. elegans* is mediated by two complementary mechanisms that act through separate PIE-1 protein domains. *Mol. Cell.* **6,** 445–455 (2000).
26. Guo, S. & Kemphues, K. J. par-1, a gene required for establishing polarity in *C. elegans* embryos, encodes a putative Ser/Thr kinase that is asymmetrically distributed. *Cell* **81,** 611–620 (1995).
27. Strome, S. & Wood, W. B. Immunofluorescence visualization of germ-line-specific cytoplasmic granules in embryos, larvae, and adults of *Caenorhabditis elegans*. *Proc. Natl Acad. Sci. USA* **79,** 1558–1562 (1982).
28. Timmons, L. & Fire, A. Specific interference by ingested dsRNA. *Nature* **395,** 854 (1998).
29. Edgar, L. G. Blastomere culture and analysis. *Methods Cell Biol.* **48,** 303–321 (1995).
30. McCarter, J., Bartlett, B., Dang, T. & Schedl, T. On the control of oocyte meiotic maturation and ovulation in *Caenorhabditis elegans*. *Dev. Biol.* **205,** 111–128 (1999).

Acknowledgements

We are grateful to A. Golden, P. Sadler, J. Schumacher and D. Shakes for their characterization of the *mat* mutants. We also thank K. O'Connell and J. White for sharing results before publication; K. Kemphues and L. Boyd for antibodies; L. Timmons and A. Fire for RNAi feeding materials; and A. Golden, P. Sadler, D. Shakes, K. Kemphues, K. O'Connell, Y. Zheng and members of the Seydoux lab for comments on the manuscript. Some strains used in this study were provided by the Caenorhabditis Genetics Center (University of Minnesota). M.R.W. was an NSF predoctoral fellow. This work was supported by grants from the Searle and Packard Foundations to G.S.

Correspondence and requests for materials should be addressed to G.S. (e-mail: gseydoux@jhmi.edu).

Flk1-positive cells derived from embryonic stem cells serve as vascular progenitors

Jun Yamashita*, Hiroshi Itoh*, Masanori Hirashima†, Minetaro Ogawa†, Satomi Nishikawa†, Takami Yurugi*, Makoto Naito‡, Kazuwa Nakao* & Shin-Ichi Nishikawa†

** Department of Medicine and Clinical Science, and † Department of Molecular Genetics, Kyoto University Graduate School of Medicine, 54 Shogoin Kawahara-cho, Sakyo-ku, Kyoto 606-8509, Japan*
‡ The Second Department of Pathology, Niigata Univeristy School of Medicine, Asahimachi-dori 1, Niigata 951-8510, Japan

Interaction between endothelial cells and mural cells (pericytes and vascular smooth muscle) is essential for vascular development and maintenance[1–4]. Endothelial cells arise from Flk1-expressing ($Flk1^+$) mesoderm cells[5], whereas mural cells are believed to derive from mesoderm, neural crest or epicardial cells and migrate to form the vessel wall[6–8]. Difficulty in preparing pure populations of these lineages has hampered dissection of the mechanisms underlying vascular formation. Here we show that $Flk1^+$ cells derived from embryonic stem cells can differentiate into both endothelial and mural cells and can reproduce the vascular organization process. Vascular endothelial growth factor promotes endothelial cell differentiation, whereas mural cells are induced by platelet-derived growth factor-BB. Vascular cells derived from $Flk1^+$ cells can organize into vessel-like structures consisting of endothelial tubes supported by mural cells in three-dimensional culture. Injection of $Flk1^+$ cells into chick embryos showed that they can incorporate as endothelial and mural cells and contribute to the developing vasculature *in vivo*. Our findings indicate that $Flk1^+$ cells can act as 'vascular progenitor cells' to form mature vessels and thus offer potential for tissue engineering of the vascular system.

Flk1, one of the receptors for vascular endothelial growth factor (VEGF), is a marker for lateral plate mesoderm[5] and the earliest differentiation marker for endothelial cells and blood cells[9,10]. We previously established an induction and purification system for $Flk1^+$ cells from embryonic stem (ES) cells and showed that $Flk1^+$ cells give rise to endothelial cells as well as blood cells *in vitro*[11–13]. To elucidate the mechanisms underlying vascular development, we